



IJRASET

International Journal For Research in
Applied Science and Engineering Technology



INTERNATIONAL JOURNAL FOR RESEARCH

IN APPLIED SCIENCE & ENGINEERING TECHNOLOGY

Volume: 4

Issue: 1

Month of publication: January 2016

DOI:

www.ijraset.com

Call:  08813907089

E-mail ID: ijraset@gmail.com

Impact of Heat Generation/Absorption on Steady MHD Boundary Layer Flow of Nanofluid over a Permeable Stretching Sheet in Porous Medium with Chemical Reaction

A. K. Pandey¹, Manoj Kumar²

^{1,2}Department of Mathematics, Statistics and Computer Science

G.B. Pant University of Agriculture and Technology, Pantnagar, Utrakhand, India-263145

Email: alokpandey1@gmail.com, mnj_kumar2004@2004

Abstract: This present paper deals with the effect of heat generation/absorption on steady magneto hydrodynamic flow of a nanofluid past a permeable stretching surface in porous medium with chemical reaction. The radiative heat flux is describe by Rosseland approximation and using in energy equation. The governing non-linear partial differential equations are transformed into a system of non-linear ordinary differential equations using similarity transformations and then solved numerically using the Runge-Kutta-Felberg method with shooting technique. The non-dimensional velocity, temperature and concentration profiles are depicted graphically for various values of physical parameters and analysed. The local skin friction coefficient, local Nusselt number and Sherwood number also discussed. It is found that volume concentration of nanoparticle increases on increasing the values of chemical reaction parameter and velocity of nanoparticle decreases with enhancing values of porosity parameter.

Keywords: Nanofluid, Porous medium, MHD, Chemical reaction, Heat generation/absorption.

2010 Mathematics Subject Classification: 80A20, 76D05, 76D10, 82D80.

I. NOMENCLATURE

B_0	magnetic field
C_f	skin-friction coefficient
C_w	volume concentration at wall
D_B	Brownian diffusion coefficient
D_T	thermophoretic diffusion coefficient
Ec	Eckert number
H	heat generatio/absorption parameter
k_1	rate of chemical reaction
k^*	mean absorption coefficient
k	thermal conductivity of the nanofluid [$Wm^{-1}K^{-1}$]
Le	Lewis number
l	length of the sheet
M	magnetic parameter
Nb	Brownian motion parameter
Nt	thermophoresis parameter
Nu	Nusselt number
Pr	Prandtl number
Q	heat generation/absorption coefficient
q_r	radiative heat flux [W/m^2]
R	thermal radiation parameter

International Journal for Research in Applied Science & Engineering Technology (IJRASET)

S	suction parameter
Sh	Sherwood number
T_w	temperature at the wall
T	temperature [K]
u, v	velocities in x,y-directions [ms^{-1}]
x, y	axial and perpendicular co-ordinates [m]
Greek Symbols	
ψ	stream function
β	thermal expansion coefficient of the base fluid
ϕ	nanoparticle volume fraction, %
η	similarity variable
γ	chemical reaction parameter
Λ	porosity parameter
$(C\rho)_f$	heat capacity of the fluid
ν	kinematic viscosity of the fluid [m^2s^{-1}]
K	thermal conductivity of the fluid [$Wm^{-1}K^{-1}$]
θ	non-dimensional temperature
α	thermal diffusivity
σ^*	Stefan–Boltzmann constant
ρ_f	density of base fluid [kgm^{-3}]
ρ_p	density of solid particle [kgm^{-3}]
Subscripts	
∞	free stream condition
w	condition at the wall
f	base fluid
p	nanoparticle
Superscript	
'	derivative with respect to η

II. INTRODUCTION

Nanofluid are the suspensions including a fluid which contain nanoparticle of average size under 100nm such as ceramics, metals, alloys and semi-conductors. They have various application such as cancer therapy, energy storage, drug delivery and vehicle brake fluids. Wubshet et al.[1] studied heat transfer of a nanofluid over a stretching sheet in the presence of MHD, thermal radiation and slip conditions. They found that on enhancing the values of magnetic parameter the nanofluid, velocity reduces and temperature of the surface decreases on enhancing the values of Prandtl number. Khan et al.[2] have discussed the effects of MHD and heat transfer on bioconvection conducting nanofluid flow in the presence of gyrotactic microorganisms over a convectively heated stretching sheet. They found that on increasing the values of magnetic parameter, the Sherwood number reduces while on enhancing stretching parameter, the Sherwood number increases. Nandy et al.[3] have discussed MHD boundary layer flow of a nanofluid over a stretching/shrinking surface in the presence of heat generation/absorption and slip with convective boundary conditions. They analyzed that on increasing the values of Brownian parameter, nanoparticle volume fraction continuously reduces for stretching surface and regularly increases with enhancing the values of thermophoresis parameter. Similarly, nanofluid flow along a permeable stretching surface in presence of natural convection and heat generation/absorption has been studied by Das[4]. The author analyzed that on enhancing the values of nanoparticle volume fraction, the velocity of nanoparticle reduces for Cu-water and temperature of nanoparticle near the boundary layer reduces with enhancing the suction parameter and increases with reducing injection parameter. Dalir et al.[5] investigated the impact of heat transfer and MHD of a nanofluid along a stretching surface in the presence of viscous dissipation. They showed that in the vicinity of the sheet entropy generation parameter increases on enhancing the values of Lewis number and Prandtl number, and on increasing the values Eckert number both temperature and volume gradient of nanoparticle increase. Hakeem et al.[6] have discussed the effects of thermal radiation and MHD on two dimensional nanofluid flow along a stretching/shrinking

International Journal for Research in Applied Science & Engineering Technology (IJRASET)

surface with slip condition. They found that in the proximity of boundary layer normal and stream wise velocity decreases on enhancing the values of magnetic parameter and nanoparticle volume fraction for stretching surface while for shrinking upper branch solution, both velocity components increase with increasing the values of magnetic parameter and nanoparticle volume fraction. Rashad et al.[7] describing the impact of mixed convection boundary layer flow past a horizontal circular cylinder embedded in a porous medium. They analyzed that on growing the values of mixed convection parameter both local Nusselt number and Sherwood number increases. Rana et al.[8] have discussed numerical investigation of nanofluid flow along an inclined plate embedded in a porous medium in the presence of mixed convection. They showed that on enhancing the values Brownian parameter, both the temperature and volume fraction of nanoparticle growing; and on growing the values of Lewis number, temperature of nanoparticle decreases and volume concentration of nanoparticle rises. Tham et al.[9] analyzed the convective heat transfer flow past a horizontal circular cylinder embedded within the porous media. They showed that on enhancing the values of Brownian parameter, Lewis number, thermophoresis parameter and heat flux reduced. Wahiduzzaman et al.[10] investigated the influence of heat generation and thermal radiation on two dimensional stagnation point flow along a shrinking surface in the presence of chemical reaction and MHD. Zhang et al.[11] studied the effects of chemical reaction and heat transfer of a nanofluid flow in porous media in the presence of surface heat flux and MHD. They found that on enhancing the values of magnetic parameter velocity of nanoparticle growing and temperature of nanoparticle increases on increasing the values of nanoparticle volume fraction. In the present study we analyzed the effects of heat generation/absorption and MHD boundary layer flow of a two dimensional nanofluid past a permeable stretching surface with in the porous media in the presence of chemical reaction, heat transfer and solutal slip boundary conditions. The equations that obtained have been solved in symbolic computation software with the help of Runge-Kutta-Felberg method and shooting technique. The effects of different physical parameters on the velocity, temperature and volume concentration are depicted graphically.

III. MAHEMATICAL FORMULATION

Suppose a steady boundary layer flow of a nanofluid flow along a stretching sheet of surface temperature T_w and volume concentration of nanoparticle C_w . The extended velocity of the sheet is $u_w = ax$. Where a is constant, V_w is mass transfer of the wall, temperature and concentration far from the sheet are T_∞, C_∞ respectively. Chosen x - axis as towards stretching sheet and y -axis as normal to the sheet.

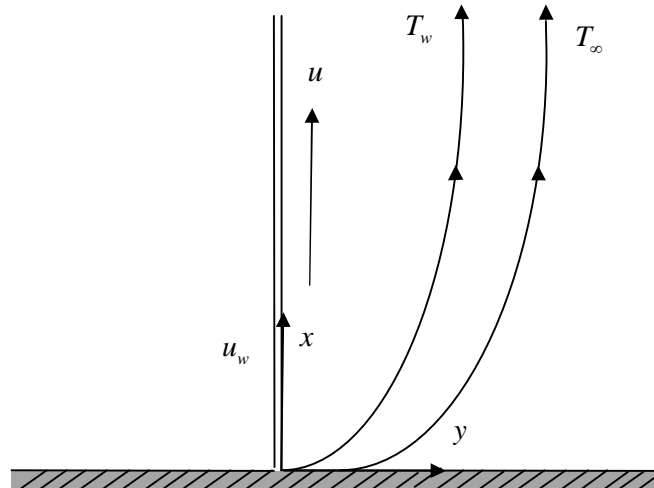


Figure 1 Physical model and coordinate system of the problem.

The governing non-linear partial differential equations are as follows:

$$\frac{\partial u}{\partial x} + \frac{\partial v}{\partial y} = 0 \tag{1}$$

$$u \frac{\partial u}{\partial x} + v \frac{\partial v}{\partial x} = -\frac{1}{\rho_f} \frac{\partial p}{\partial x} + \nu \left(\frac{\partial^2 u}{\partial x^2} + \frac{\partial^2 u}{\partial y^2} \right) - \frac{\sigma B_0^2}{\rho_f} u + \frac{\nu}{k} (U(x) - u) \tag{2}$$

International Journal for Research in Applied Science & Engineering Technology (IJRASET)

$$u \frac{\partial u}{\partial x} + v \frac{\partial v}{\partial y} = -\frac{1}{\rho_f} \frac{\partial p}{\partial y} + v \left(\frac{\partial^2 v}{\partial x^2} + \frac{\partial^2 v}{\partial y^2} \right) - \frac{\sigma B_0^2}{\rho_f} v \quad (3)$$

$$u \frac{\partial T}{\partial x} + v \frac{\partial T}{\partial y} = \alpha \left(\frac{\partial^2 T}{\partial x^2} + \frac{\partial^2 T}{\partial y^2} \right) - \frac{1}{(\rho C)_f} \frac{\partial q_r}{\partial y} + \frac{\mu}{\rho C_p} \left(\frac{\partial u}{\partial y} \right)^2 + \left(\frac{\sigma B_0^2}{\rho C_p} \right) u^2 + \tau \left\{ D_B \left(\frac{\partial C}{\partial x} \frac{\partial T}{\partial x} + \frac{\partial C}{\partial y} \frac{\partial T}{\partial y} \right) + \frac{D_T}{T_\infty} \left[\left(\frac{\partial T}{\partial x} \right)^2 + \left(\frac{\partial T}{\partial y} \right)^2 \right] \right\} + \frac{Q}{\rho C_p} (T - T_\infty) \quad (4)$$

$$u \frac{\partial C}{\partial x} + v \frac{\partial C}{\partial y} = D_B \left(\frac{\partial^2 C}{\partial x^2} + \frac{\partial^2 C}{\partial y^2} \right) + \frac{D_T}{T_\infty} \left(\frac{\partial^2 T}{\partial x^2} + \frac{\partial^2 T}{\partial y^2} \right) - k_1 (C - C_\infty) \quad (5)$$

Where $\rho_f, \sigma, B_0, \rho_p, (\rho C)_f, D_B, D_T, k_1$ and Q are the density of the base fluid, electrical conductivity, magnetic field, the density of the nanoparticle, heat capacity of a fluid, Brownian diffusion and thermophoresis diffusion coefficient, rate of chemical reaction and heat generation/absorption coefficient.

The related boundary conditions are

$$u = u_w + L \frac{\partial u}{\partial y}, v = V_w, T = T_w + K_1 \frac{\partial T}{\partial y}, C = C_w + K_2 \frac{\partial C}{\partial y}, \text{ at } y = 0 \quad (6)$$

$$u \rightarrow U_\infty = 0, T \rightarrow T_\infty, C \rightarrow C_\infty, \text{ as } y \rightarrow \infty$$

Where $u_w = ax, T_w = T_\infty + b \left(\frac{x}{l} \right)^2, C_w = C_\infty + c \left(\frac{x}{l} \right)^2, L, K_1, K_2$ and l are velocity, thermal and concentration slip factor, length of sheet respectively, and if velocity, thermal and concentration slip factor are absent then slip condition not occurs All the above boundary conditions are true

when $x \ll l$ which exist closed to the slit. Taking magnitude analysis of the y-direction momentum equation (normal to the sheet) with general boundary layer adjacency, such as:

$u \ll v$

$$\frac{\partial u}{\partial y} \ll \frac{\partial u}{\partial x}, \frac{\partial v}{\partial x}, \frac{\partial v}{\partial y} \quad (7)$$

$$\frac{\partial p}{\partial y} = 0$$

With the help of boundary-layer adjacency, the governing equations are converted into :

$$\frac{\partial u}{\partial x} + \frac{\partial v}{\partial y} = 0 \quad (8)$$

$$u \frac{\partial u}{\partial x} + v \frac{\partial v}{\partial x} = v \left(\frac{\partial^2 u}{\partial y^2} \right) - \frac{\sigma B_0^2}{\rho_f} u + \frac{v}{k} (U(x) - u) \quad (9)$$

$$u \frac{\partial T}{\partial x} + v \frac{\partial T}{\partial y} = \alpha \left(\frac{\partial^2 T}{\partial y^2} \right) - \frac{1}{(\rho C)_f} \left(\frac{\partial q_r}{\partial y} \right) + \frac{\mu}{(\rho C)_p} \left(\frac{\partial u}{\partial y} \right)^2 + \left(\frac{\sigma B_0^2}{\rho C_p} \right) u^2 + \frac{Q}{\rho C_p} (T - T_\infty) + \tau \left[D_B \frac{\partial C}{\partial y} \frac{\partial T}{\partial y} + \frac{D_T}{T_\infty} \left(\frac{\partial T}{\partial y} \right)^2 \right] \quad (10)$$

International Journal for Research in Applied Science & Engineering Technology (IJRASET)

$$u \frac{\partial C}{\partial x} + v \frac{\partial C}{\partial y} = D_B \left(\frac{\partial^2 C}{\partial x^2} + \frac{\partial^2 C}{\partial y^2} \right) + \frac{D_T}{T_\infty} \left(\frac{\partial^2 T}{\partial x^2} + \frac{\partial^2 T}{\partial y^2} \right) - k_1 (C - C_\infty) \quad (11)$$

The relevant boundary conditions are:

$$u = u_w + L \frac{\partial u}{\partial y}, \quad v = V_w, \quad T = T_w + K_1 \frac{\partial T}{\partial y}, \quad C = C_w + K_2 \frac{\partial C}{\partial y}, \quad \text{at } y = 0 \quad (12)$$

$$u \rightarrow U_\infty = 0, \quad T \rightarrow T_\infty, \quad C \rightarrow C_\infty \text{ as } y \rightarrow \infty$$

Where $\alpha = \frac{k}{(C\rho)_f}$, $\tau = \frac{(C\rho)_p}{(C\rho)_f}$, $\nu = \frac{\mu}{\rho_f}$, x and y represent coordinate axes. The velocity along x and y axis are u and v

respectively. Further ν is the kinematic viscosity, ρ is the density, T is the temperature $(\rho C)_p$ is the effective heat capacity of the nanofluid particle, T_∞ and C_∞ are the ambient temperature and concentration respectively.

Equations (8) – (11) are transformed into a set of non-linear ordinary differential equations by using the following similarity variables:

$$\eta = \sqrt{\frac{a}{\nu}} y, \quad \psi = \sqrt{a\nu} x f(\eta), \quad \theta(\eta) = \frac{T - T_\infty}{T_w - T_\infty}, \quad \phi(\eta) = \frac{C - C_\infty}{C_w - C_\infty}. \quad (13)$$

In usual way a stream function $\psi(x, y)$ is defined as

$$u = \frac{\partial \psi}{\partial y} \quad \text{and} \quad v = -\frac{\partial \psi}{\partial x}. \quad (14)$$

With the help of Rosseland approximation, the radiative heat flux is

$$q_r = -\frac{4\sigma^*}{3k^*} \frac{\partial T^4}{\partial y} \quad (15)$$

Where σ^* is the Stefan-Boltzman constant and k^* is the mean absorption coefficient, and T^4 is the linear sum of temperature and it can be expand with help of Taylor series about T_∞ .

$$T^4 = T_\infty^4 + 4T_\infty^3 (T - T_\infty) + 6T_\infty^2 (T - T_\infty)^2 + \dots \quad (16)$$

Ignoring higher terms of $(T - T_\infty)$ onwards of eqs. (16) we get:

$$T^4 \cong 4T_\infty^3 T - 3T_\infty^4 \quad (17)$$

Solving eqs.(15) and (17) we get:

$$q_r = -\frac{16T_\infty^3 \sigma^*}{3k^*} \frac{\partial T}{\partial y} \quad (18)$$

The transformed ordinary differential equations are :

$$f''' + ff'' - f'^2 - Mf' - \Lambda f' = 0. \quad (19)$$

$$\left(1 + \frac{4}{3}R\right)\theta'' + \text{Pr} f\theta' - 2\text{Pr} f'\theta + \text{Pr} Ecf'' + \text{Pr} MEcf'^2 + \text{Pr} Nb\theta'\phi' + \text{Pr} Nt\theta'^2 + \text{Pr} H\theta = 0. \quad (20)$$

$$\phi'' + \text{Le}f\phi' - 2\text{Le}f'\phi + \frac{Nt}{Nb}\theta'' - \gamma\phi = 0. \quad (21)$$

Associated boundary conditions are :

$$f(0) = S, \quad f'(0) = 1 + Af''(0), \quad \theta(0) = 1 + B\theta'(0), \quad \phi(0) = 1 + C\phi'(0), \quad \text{at } \eta = 0$$

$$f'(\infty) = 0, \quad \theta(\infty) = 0, \quad \phi(\infty) = 0 \quad \text{as } \eta \rightarrow \infty. \quad (22)$$

International Journal for Research in Applied Science & Engineering Technology (IJRASET)

Where the governing parameters are

$$Pr = \frac{\nu}{\alpha}, Ec = \frac{u_w^2}{C_p (T_w - T_\infty)}, R = \frac{4\sigma^* T_\infty^3}{k^* k}, M = \frac{\sigma B_0^2}{\rho_f a}, Nb = \frac{(\rho C)_p D_B (C_w - C_\infty)}{(\rho C)_f \nu}, Nt = \frac{(\rho C)_p D_T (T_w - T_\infty)}{(\rho C)_f \nu T_\infty},$$

$$Le = \frac{\nu}{D_B}, \Lambda = \frac{\nu}{\kappa}, H = \frac{Q}{a \rho C_p}, \gamma = \frac{k_1 \nu}{a}, A = L \sqrt{\frac{a}{\nu}},$$

$$B = K_1 \sqrt{\frac{a}{\nu}}, C = K_2 \sqrt{\frac{a}{\nu}}. \tag{23}$$

where Nt is thermophoresis parameter, Nb is the Brownian parameter, H is the heat generation/absorption parameter, Λ is the porosity parameter, γ is chemical reaction parameter, R is the radiation parameter, M is the magnetic field parameter, Le is the Lewis number, Pr is the Prandtl number, Ec is the Eckert number, S is the suction parameter and A, B, C are the velocity, thermal and concentration slip parameters, respectively :

For the practical interest, skin friction coefficient C_f , Nusselt number Nu and Sherwood number Sh are defined as

$$C_f = \frac{\mu}{\rho_f u_w^2} \left(\frac{\partial u}{\partial y} \right)_{y=0} = -Re_x^{-1/2} f'' ,$$

$$Nu = -\frac{x}{T_w - T_\infty} \left(\frac{\partial T}{\partial y} \right)_{y=0} = -(1+R) Re_x^{1/2} \theta'(0), \quad Sh = -\frac{x}{C_w - C_\infty} \left(\frac{\partial C}{\partial y} \right)_{y=0} = -Re_x^{1/2} \phi'(0).$$

Where $Re_x = \frac{x u_w}{\nu_f}$ is the local Reynolds number. The reduced skin friction coefficient, reduced Nusselt number and reduced

Sherwood number are denoted as

$$Re_x^{1/2} C_f = -f''(0), \quad Nur = Re_x^{-1/2} Nu = -(1+R)\theta'(0), \quad \text{and} \quad Shr = Re_x^{-1/2} Sh = -\phi'(0). \tag{24}$$

IV. RESULTS AND DISCUSSION

In order to study the effects of the porosity parameter Λ , heat generation/absorption parameter H and chemical reaction parameter γ , the other dimensionless parameters are fixed as $Ec = 0.2, Pr = 1, R = 0.5, M = 0.5, Nb = 0.1, Nt = 0.2, Le = 5.0, A = B = C = 1$. Then the non-dimensional velocity, temperature and concentration profiles are illustrated in Figures 1-6. The variation of three physical parameters with different values of porosity parameter are shown in Table 1. It is seen from table that on increasing the values of Λ , reduced skin friction coefficient increases and both reduced Nusselt and Sherwood number reduces. The effects of heat generation/absorption parameter is shown in Table 2. We notice that from this table when increasing the values of H , reduced Nusselt number decreases and mass transfer rate increases and Table 3 illustrate that on increasing the values of chemical reaction parameter γ mass transfer rate reduces.

Table 1

Variation of the reduced skin friction coefficient, the reduced Nusselt number and reduced Sherwood number in the case of $Ec = Nt = 0.2, M = R = S = 0.5, Nb = 0.1, Le = 5, H = 0, \gamma = 0$.

Λ	$-f''(0)$	$-\theta'(0)$	$-\phi'(0)$
0.1	0.597921	0.35957	0.68343
0.2	0.634332	0.28983	0.67433
0.3	0.665962	0.18877	0.45083
0.4	0.693692	0.04580	0.43940

International Journal for Research in Applied Science & Engineering Technology (IJRASET)

Table 2

Variation of the reduced Nusselt number and reduced Sherwood number in the case of $Ec = Nt = 0.2$, $M = R = S = 0.5$, $Nb = 0.1$, $Le = 5$, $\Lambda = 0$, $\gamma = 0$.

H	$-\theta'(0)$	$-\phi'(0)$
-3.0	0.60128	0.73736
-2.0	0.5595	0.81000
-1.0	0.4884	0.96539
1.0	0.35689	4.48604
1.3	0.16098	6.24146

Table 3

Variation of the reduced Sherwood number in the case of $Ec = Nt = 0.2$, $M = R = S = 0.5$, $Nb = 0.1$, $Le = 5$, $\Lambda = 0$, $H = 0$.

γ	$-\phi'(0)$
0.5	0.92680433
1.0	0.81390433
1.5	0.79136433
2.5	0.78244693

Fig.2 depicts that the effect of porosity parameter Λ on fluid velocity. These figures show that on increasing the values of Λ the velocity of nanoparticle regularly decreases then the boundary layer thickness of velocity reduces. Fig.3 reveals that on increasing the values of porosity parameter Λ , temperature of the nanoparticle increases. Due to this reason thermal boundary layer thickness increases and surface temperature also growing. Fig.4 demonstrates the impact of porosity parameter Λ on nanoparticle volume concentration ϕ . It is observed from graph that on enhancing the values of porosity parameter Λ the concentration of nanoparticle increases. Due to this reason concentration boundary layer thickness become large. The influence of heat generation/absorption parameter H on temperature and concentration are shown in Figs 5-6. Fig.5 illustrates that on increasing the values of heat absorption temperature of nanoparticle continuously increases and on enhancing the values of heat generation temperature of nanoparticle growing near the sheet then after far from sheet it reduces. Fig.6 reveals that on enhancing the values of heat absorption parameter concentration of nanoparticle near the vicinity of surface decreases and far from the surface there is no variation in concentration boundary layer thickness and on growing the values of heat generation parameter concentration of nanoparticle significantly decreases. Due to this reason concentration of boundary layer thickness reduces. The impact of chemical reaction parameter on nanoparticle concentration shown in Fig.7. It is seen that on increasing the values of chemical reaction parameter nanoparticle volume concentration significantly enhancing. The reason for this is that fact nanoparticle concentration boundary layer becomes thick.

International Journal for Research in Applied Science & Engineering Technology (IJRASET)

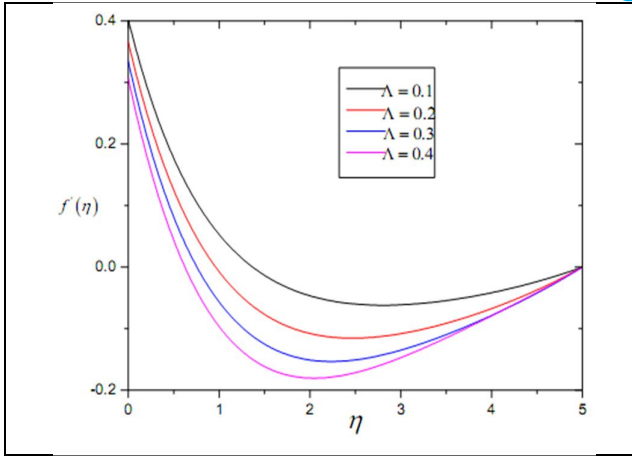


Fig.2. Velocity profiles of various values of porosity parameter Λ when $Ec = Nt = 0.2$, $M = R = S = 0.5$, $Nb = 0.1$, $Le = 5$, $H = 0$, $\gamma = 0$.

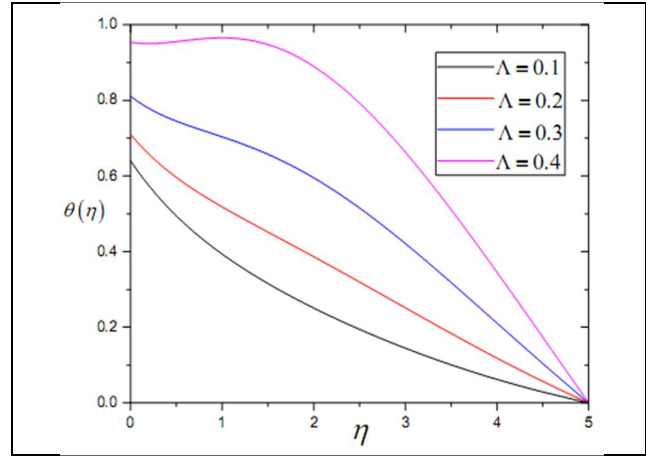


Fig.3. Temperature profiles of various values of porosity parameter Λ when $Ec = Nt = 0.2$, $M = R = S = 0.5$, $Nb = 0.1$, $Le = 5$, $H = 0$, $\gamma = 0$.

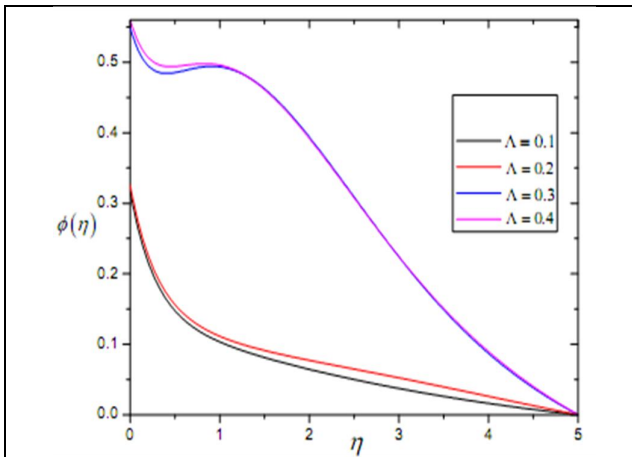


Fig.4. Concentration profiles of various values of porosity parameter Λ when $Ec = Nt = 0.2$, $M = R = S = 0.5$, $Nb = 0.1$, $Le = 5$, $H = 0$, $\gamma = 0$.

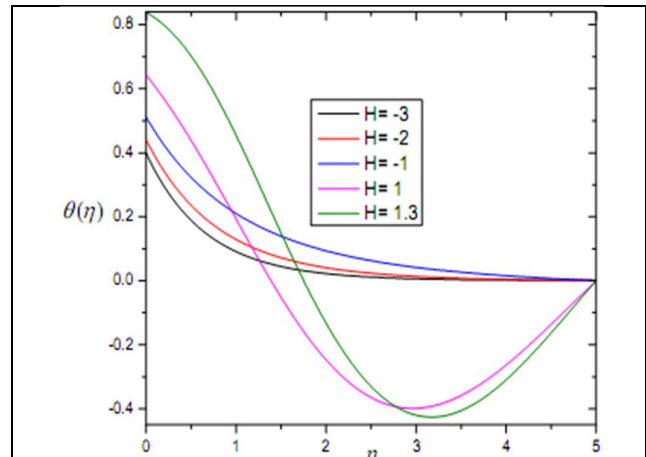


Fig.5. Temperature profiles of various values of heat generation/absorption parameter H when $Ec = Nt = 0.2$, $M = R = S = 0.5$, $Nb = 0.1$, $Le = 5$, $\Lambda = 0.3$, $\gamma = 0$.

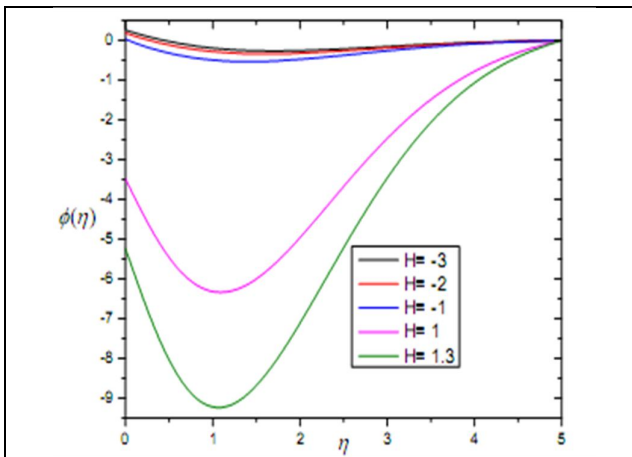


Fig.6. Concentration profiles of various values of heat generation/absorption parameter H when $Ec = Nt = 0.2$, $M = R = S = 0.5$, $Nb = 0.1$, $Le = 5$, $\Lambda = 0.3$, $\gamma = 0$.

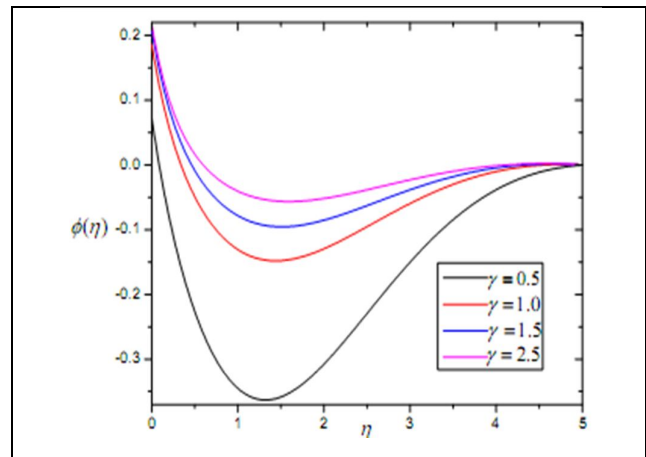


Fig.7. Concentration profiles of various values of chemical reaction parameter γ when $Ec = Nt = 0.2$, $M = R = S = 0.5$, $Nb = 0.1$, $Le = 5$, $\Lambda = 0.3$,

International Journal for Research in Applied Science & Engineering Technology (IJRASET)

V. CONCLUSIONS

The impact of various governing parameters like porosity parameter Λ , heat generation/absorption parameter H , chemical reaction parameter γ on steady MHD flow of a nanofluid past a permeable stretching surface in porous medium in the presence of heat generation/absorption and chemical reaction. The dimensionless parameters velocity, temperature and concentration profiles are studied. Thus, the following conclusion were obtained:

- A. On increasing the values of porosity parameter Λ the velocity of nanoparticle significantly decreases and temperature of the nanoparticle rises.
- B. On enhancing the values of heat generation parameter H , nanoparticle volume concentration reduces.
- C. The volume concentration of nanoparticle increases, while on increasing the values of chemical reaction parameters γ .
- D. Heat and mass transfer rate decreases with increasing in porosity parameter Λ while sheare stress rate rises with increasing in porosity parameter Λ .
- E. Mass transfer rate decreases with increasing in chemical reaction parameter γ .

REFERENCES

- [1] Wubshet I., Bandari S., MHD boundary layer flow and heat transfer of a nanofluid past permeable stretching sheet with velocity, thermal and solutal slip boundary conditions, *Computers & Fluids*, vol. 75, pp. 1–10, 2013.
- [2] Khan W.A., Makinde O.D., MHD nanofluid bioconvection due to gyrotactic microorganisms over a convectively heat stretching sheet, *International Journal of Thermal Sciences*, vol.81, pp. 118-124, 2014.
- [3] Nandy S. K., Mahapatra T. R., Effects of slip and heat generation/absorption on MHD stagnation flow of nanofluid past a stretching/shrinking surface with convective boundary conditions, *International Journal of Heat and Mass Transfer*, vol. 64 .pp. 1091–1100, 2013.
- [4] Das K., Slip flow and convective heat transfer of nanofluids over a permeable Stretching surface, *Computers & Fluids*, vol. 64, pp. 34–42, 2012.
- [5] Dalir N., Dehsara M. , Nourazar S. S., Entropy analysis for magnetohydrodynamic flow and heat transfer of a Jeffrey nanofluid over a stretching sheet, *Energy*, vol. 79 , pp. 351- 362, 2015.
- [6] Hakeem A. K. A. , Ganesh N. V. , Ganga B. , Magnetic field effect on second order slip flow of nanofluid over a stretching/shrinking sheet with thermal radiation effect, *Journal of Magnetism and Magnetic Materials*, vol. 381, pp. 243–257, 2015.
- [7] Rashad A.M., Chamkha A.J., Modather M., Mixed convection boundary-layer flow past a horizontal circular cylinder embedded in a porous medium filled with a nanofluid under convective boundary condition, *Computers & Fluids*, vol. 86, pp. 380–388, 2013.
- [8] Rana P., Bhargava R. , Bég O.A., Numerical solution for mixed convection boundary layer flow of a nanofluid along an inclined plate embedded in a porous medium, *Computers and Mathematics with Applications*, vol. 64, pp. 2816–2832, 2012.
- [9] Tham L., Nazar R., Pop I., Mixed convection flow from a horizontal circular cylinder embedded in a porous medium filled by a nanofluid: Buongiornoe Darcy model, *International Journal of Thermal Sciences*, vol. 84, pp. 21-33, 2014.
- [10] Wahiduzzaman M., Khan Md. S., Karim I., MHD Convective Stagnation Flow of Nanofluid over a Shrinking Surface with Thermal Radiation, Heat Generation and Chemical Reaction, *Procedia Engineering*, vol. 105, pp. 398 – 405, 2015.
- [11] Zhang C., Zheng L., Zhang X., Chen G., heat transfer of a nanofluid flow in a porous media in the presence of MHD, chemical reaction and surface heat flux, *Applied Mathematical Modelling*, vol. 39, pp. 165–181, 2015.



10.22214/IJRASET



45.98



IMPACT FACTOR:
7.129



IMPACT FACTOR:
7.429



INTERNATIONAL JOURNAL FOR RESEARCH

IN APPLIED SCIENCE & ENGINEERING TECHNOLOGY

Call : 08813907089  (24*7 Support on Whatsapp)